UNIVERSITY *of* York

This is a repository copy of *Effect of annealing on the structure and magnetic properties of Co2FeAl0.5Si0.5 thin films on Ge(111)*.

White Rose Research Online URL for this paper:
https://eprints.whiterose.ac.uk/128493/

Version: Accepted Version

Article:

Kuerbanjiang, Balati orcid.org/0000-0001-6446-8209, Love, Christopher, Kepaptsoglou, Demie orcid.org/0000-0003-0499-0470 et al. (7 more authors) (2018) Effect of annealing on the structure and magnetic properties of Co2FeAl0.5Si0.5 thin films on Ge(111). JOURNAL OF ALLOYS AND COMPOUNDS. ISSN 0925-8388

White Rose
university consortium
Universities of Leeds, Sheffield & York

eprints@whiterose.ac.uk
https://eprints.whiterose.ac.uk/

Accepted Manuscript

Effect of annealing on the structure and magnetic properties of $Co_2FeAl_{0.5}Si_{0.5}$ thin films on Ge(111)

Balati Kuerbanjiang, Christopher Love, Demie Kepaptsoglou, Zlatko Nedelkoski, Shinya Yamada, Arsham Ghasemi, Quentin M. Ramasse, Kohei Hamaya, Stuart A. Cavill, Vlado K. Lazarov

Please cite this article as: B. Kuerbanjiang, C. Love, D. Kepaptsoglou, Z. Nedelkoski, S. Yamada, A. Ghasemi, Q.M. Ramasse, K. Hamaya, S.A. Cavill, V.K. Lazarov, Effect of annealing on the structure and magnetic properties of $Co_2FeAl_{0.5}Si_{0.5}$ thin films on Ge(111), *Journal of Alloys and Compounds* (2018), doi: 10.1016/j.jallcom.2018.03.075.

Effect of annealing on the structure and magnetic properties of $Co_2FeAl_{0.5}Si_{0.5}$ thin films on Ge(111)

Balati Kuerbanjiang[1], Christopher Love[1,2], Demie Kepaptsoglou[3], Zlatko Nedelkoski[1], Shinya Yamada[4], Arsham Ghasemi[1], Quentin M. Ramasse[3], Kohei Hamaya[4], Stuart. A. Cavill[1,2] and Vlado K. Lazarov[1*]

[1]Department of Physics, University of York, York YO10 5DD, UK
[2]Diamond Light Source, Harwell Science and Innovation Campus, Didcot, OX11 0DE, UK
[3]SuperSTEM Laboratory, SciTech Daresbury Campus, Daresbury WA4 4AD, UK
[4]Department of Systems Innovation, Osaka University, Osaka 560-8531, Japan

*email: vlado.lazarov@york.ac.uk

Abstract:

We present a magnetic and structural properties study of epitaxially grown *B*2-ordered full Heusler $Co_2FeSi_{0.5}Al_{0.5}$ single crystal films on Ge(111) substrates, as a function of annealing temperature. Hysteresis loop measurements reveal that the magnetic properties of $Co_2FeSi_{0.5}Al_{0.5}$ are stable up to 450 °C while ferromagnetic resonance linewidth measurements show a reduction of Gilbert damping from 5.6×10^{-3} to 2.9×10^{-3} for as-grown and annealed film, respectively. Above 500 °C, the films have increased coercivity, decreased saturation magnetization, and show characteristic two-magnon scattering resonance line-shapes. Magnetic inhomogeneities developed within the film when annealed above 500 °C were correlated to significant interdiffusion at the film-substrate interface, as confirmed by scanning transmission electron microscopy and electron energy loss spectroscopy. By performing first-principles calculations based on atomistic models developed from atomically-resolved microscopy images, we show the magnetic moment of the $Co_2FeSi_{0.5}Al_{0.5}$ film reduces upon Co substitution by Ge atoms.

1. Introduction

Efficient spin-injection from half-metallic ferromagnets into semiconductors is crucial for the development of hybrid spintronic devices such as spin transistors [1-4]. Half-metallic ferromagnets such as Co-based full Heusler alloys that are 100% spin-polarized at the Fermi-level are ideal candidates for such devices [5-8]. In particular, $Co_2FeSi_{0.5}Al_{0.5}$ (CFAS) shows great promise due to its high Curie temperature, high magnetic moment, mid-gap Fermi level, and low Gilbert damping constant [9-14]. In addition to its thermal stability, CFAS has excellent lattice match with Ge (only ~0.4% lattice mismatch). Furthermore, in comparison to the CFAS/Si interface previously investigated by our group [5], recent studies show that the CFAS/Ge interface preserves both the high spin-polarization of the CFAS film as well as its magnetic moment in the interface vicinity, making this system an excellent platform for spin-based device applications [5, 6].

Despite the predicted ideal properties of fully ordered $L2_1$ single crystal half-metallic Heusler alloys, structural defects and chemical disorder can drastically change the spin polarisation [7, 15, 16] in Heusler thin films. In order to improve spin-electronic properties, thermal treatment is essential not only to remove the point- and extended structural defects but also to achieve the chemically-ordered $L2_1$ phase throughout the film [17, 18]. Annealing at elevated temperatures in the range of 500-700 °C is a standard approach undertaken for various heterostructures such as CPP-SVs and MTJs based on half-metallic Heusler electrodes [11, 15, 19, 20]. In the case of hybrid heterostructures, annealing at such relatively high temperatures presents a large barrier for improving the film properties due to an extensive intermixing between the semiconducting substrate and Heusler film which usually occurs even at lower temperatures. In contrast to CFAS/Si where extensive intermixing has been observed even for room temperature deposition [5], recent studies of CFAS films on Ge(111) have demonstrated atomically and chemically sharp interfaces for room temperature deposition [6]. The structural phase of the room temperature deposited CFAS is $B2$ and defects such as antiphase boundaries, which locally destroy the spin polarisation, have been observed [7]. Therefore, it is important to determine how the annealing affects overall film structure as well as the atomic and chemical structure of the CFAS/Ge interface. Keeping the structural and chemical integrity of the half-metal/semiconductor interface is crucial since it determines the heterostructure band alignment, Schottky barrier height and ultimately the spin injection efficiency.

In this letter, we present a systematic study of the effect of annealing temperature on the CFAS/Ge heterostructure with a goal of establishing a correlation between structure, magnetic properties and interface integrity in the temperature range from 350-550 °C. Vibrating sample magnetometer (VSM) measurements show stable overall magnetisation and film coercivity up to 450 °C. The decrease of the Gilbert damping constant, measured by ferromagnetic resonance (FMR), within the same temperature range indicates improved structural/chemical ordering of the CFAS film. A further increase in the annealing temperature results in an increase of resonance linewidth suggesting secondary magnetic phase formations, which is also reflected in a decrease of magnetisation and an increase of coercivity of the film. Aberration-corrected scanning transmission electron microscopy (STEM) and electron energy loss spectroscopy (EELS) measurements reveal that the changes in magnetic properties of the CFAS film are correlated to structural changes, mainly as a result of an interdiffusion between the Ge substrate and the CFAS film. Based on the structural data obtained by electron microscopy, we also perform first-principles calculations which correlate the drop of observed magnetisation with the structure of the annealed specimens. This work clearly shows that forming the $L2_1$ phase on Ge substrates is hindered by the strong interdiffusion of the Ge and the Heusler film. Hence the standard annealing procedures that require annealing above 500 °C are not suitable for hybrid spintronic structures.

2. Experimental

The samples were prepared by co-deposition of Co, Fe, Si and Al using low-temperature molecular beam epitaxy [21, 22]. A 18 nm-thick CFAS film was deposited on a pre-cleaned 10×10 mm^2 Ge (111) substrate at room temperature. Prior to loading Ge(111) substrates into the chamber, their surfaces were chemically cleaned with an aqueous 1% HF solution to remove any native oxide and contamination. Annealing experiments were carried out inside a UHV chamber with a base pressure of 8×10^{-11} mbar. Each 3×3 mm^2 cut sample was annealed under the same condition for an hour at a given temperature.

Cross-sectional transmission electron microscopy samples were prepared by conventional ion-thinning method. Selective area electron diffraction (SAED) patterns were recorded using a JEOL-2011 transmission electron microscope (TEM) operated at 200 kV. Atomic-level structural studies were performed by high-angle annular dark-field (HAADF) STEM imaging on a Nion UltraSTEM 100 microscope, operated at 100 kV, with a convergence angle of 30 mrad; at these optical conditions the electron probe size is determined to be 0.9 Å; the inner detector angle for HAADF STEM imaging and the EELS collection angle were 76 mrad and 32 mrad, respectively. The native energy spread of the electron beam for the EELS measurements was 0.3 eV; with the spectrometer dispersion set at 1 eV/channel. EELS chemical maps were generated from 2D-spectrum images after denoising by Principle Component Analysis, using the HREM Research MSA [23] for Digital Micrograph by integrating the signal above the relevant ionisation edge onset over a 30 eV window, after subtraction of the decaying background using a power-law model.

Density functional theory (DFT) calculations were performed with the CASTEP code [24]. The PBE+U exchange-correlation functional was used, and a Hubbard-U term set to 2.1 eV for both d-block elements Co and Fe. This value for the Hubbard-U term has previously been shown to open up the minority band-gap, approximately correcting for the delocalising effect of self-interaction with PBE alone [25]. The plane wave cut-off energy was set to 600 eV, while the Brillouin zone was sampled using a Monkhorst-Pack grid with a k-point sampling spacing of 0.035 $2\pi\text{Å}^{-1}$.

DMS model 10 VSM was used for recording hysteresis loops. A custom VNA-FMR system built around a Rohde and Schwarz Vector Network Analyser (ZNB20) was used for collecting resonance spectra using both field sweep and frequency sweep modes.

3. Results and discussion

Fig. 1(a) is an overview of the as-grown film, showing a well-defined interface with the Ge substrate. The SAED pattern (not shown) taken from a region including both the Ge(111) substrate and CFAS film demonstrates that the as-grown film is a single crystal structure; it also reveals the epitaxial crystallographic relationship between the film and substrate: CFAS(111)||Ge(111) and CFAS(1$\bar{1}$0)||Ge($\bar{1}$10). **Fig. 1(b)** is a HAADF STEM image, showing a detailed view of the interface region, where the CFAS film is observed along [1$\bar{1}$0] zone axis. The arrangement of the atomic columns confirms that CFAS film is *B*2 phase.

Next we proceed with presenting the magnetic properties of the films as a function of the annealing temperature. The films were annealed at 350 °C, 450 °C, 475 °C, 500 °C, 525 °C and 550 °C. The initial condition prior to all annealing treatment was the same, starting from as-prepared *B*2 structured films at room temperature. The magnitude of magnetisation, coercivity as well as Gilbert damping coefficient of the films depend on the chemical and structural ordering of the films. To find

the changes in magnetic properties of CFAS, in-plane magnetisation versus applied field hysteresis loops were measured using VSM. **Fig. 2** shows the values of coercivity (H_C) and saturation magnetisation (M_S) of annealed $Co_2FeAl_{0.5}Si_{0.5}$ films on Ge(111) substrates, extracted from in-plane hysteresis loops, at a range of anneal temperatures. A stable saturation magnetisation is observed up to 450 °C, followed by a continuous decrease of magnetisation with temperature. The value of H_C remains approximately constant up to 500 °C, and above this annealing temperature it increases from 7 ± 2 Oe to 60 ± 3 Oe at 550 °C. These results indicate that starting from 450 °C onwards the film undergoes structural and chemical changes which are more pronounced at higher annealing temperatures.

In order to gain further information on the changes in the magnetic properties with annealing temperature, Vector Network Analyser (VNA) ferromagnetic resonance measurements were carried out on all samples. A 2D resonance map was obtained by measuring the s-wave parameter S_{12} as a function of frequency and applied field. FMR provides information on the Gilbert damping parameter, α, from the linearly fitted slopes of the measured resonant field line width vs frequency. **Fig. 3** shows the resonant field linewidth dependence on frequency for the as-grown (a) and annealed samples (b-e). The frequency dependent linewidth, $\Delta H(f)$ is related to the damping parameter, α, by [26]

$$\Delta H(f) = \Delta H(0) + \frac{2\pi\alpha f}{\gamma} \tag{1}$$

where γ is the gyromagnetic ratio. From linear fits to the plots in **Fig. 3** using **Eq**. (1) we are able to extract both the intrinsic damping, α, and the extrinsic damping, ΔH_0, as a function of anneal temperature.

The Gilbert damping parameter, α, decreases for both the 350 °C and 450 °C annealed samples, $\alpha = 3.8 \times 10^{-3}$ and 2.9×10^{-3} respectively, compared to the as-grown sample, $\alpha = 5.6 \times 10^{-3}$, whilst the extrinsic damping remains approximately constant. The sample annealed at 450 °C shows a Gilbert damping parameter 2-3 times smaller than that of Permalloy [27, 28] and compares well to values found in the literature for CFAS and other full Heusler films [29, 30]. Above 500 °C, the line width vs frequency data shows a characteristic two-magnon scattering line-shape indicating magnetic inhomogeneities likely due to the presence of mixed magnetic phases within the sample. The FMR of the sample annealed at 550°C became very noisy due to a decreased magnetically active volume.

To understand the change of magnetic properties described above, in correlation with the annealed film structures, we performed aberration-corrected STEM imaging and elemental mapping of the annealed films. **Fig. 4** shows HAADF STEM images and corresponding EELS chemical maps of the Co $L_{2,3}$ and Ge $L_{2,3}$ edges (presented in a false coloured RGB overlay for reading clarity) from samples in the as-prepared state (a), after annealing at (b) 350 °C, (c) 500 °C and (d) 550 °C. Comparing **Fig. 4 (a)** and **(b),** there is no discernible change of the interfacial atomic structure between the RT grown and 350 °C annealed films, though in both cases the onset of Ge mixing with the CFAS film can be observed. As indicated by the magnetic measurements, the drastic changes in magnetic properties appear at 500 °C. **Fig. 4(c)** clearly shows the origin of such behaviour; the interdiffusion of Ge and CFAS film is intensified and as a result a Ge rich secondary phase with ~3 nm thickness at the interface is formed. This thickness accounts for 18% of the total initial film thickness, in line with the magnetisation reduction of the same sample (10 % drop in magnetisation). The further increase of the annealing temperature (e.g. 550 °C) increases the intermixing Ge-CFAS region as shown in **Fig. 4(d);** the depth of the secondary phase increases to around 14 ± 1 nm (~82% of the initial film thickness). We note that the reduction of the magnetisation is around 50%, indicating that the intermixed phase is magnetically inhomogeneous and in average has significantly lower

magnetisation than CFAS, *i.e.* a lower magnetic moment per formula unit. In addition, the total thickness of the film increases from ~18 nm to 24 nm after annealing at 500°C, and to 27 nm after annealing at 550°C due to heavy intermixing (see **Supp. Fig. S1**). Integrated elemental distribution profiles of Co and Ge across the interface from corresponding EELS maps are given in **Supp. Fig. S2**, where the signature of intermixing can be clearly seen by the reduction of Co and Ge signal intensities at the interface.

In order to provide some insights into how the magnetic moment per unit cell of CFAS changes with substitution of Fe-Al/Si and Co with progressive integration of Ge into the structure, we performed DFT calculations. For relatively small outdiffusion of Ge, *i.e.* for non-annealed specimens, it has been shown [6] that Ge substitutes Fe-Si/Al atoms in the Heusler film, due to the low energy of such a substitution. However, for an increased presence of Ge into the film, as observed for the specimens analysed in this work, a substitution of Ge atoms on Co sub-lattices is expected. While in Ref. [6] it has been shown that the outdiffusion of Ge into the Fe-Si/Al sub-lattice does not considerably modify the magnetic moment (unless only Fe atomic positions in unit cell are substituted by Ge), here we show that when Ge substitutes Co atoms the magnetic moment is drastically affected, **Table 1**. We consider five configurations where Ge atoms gradually replace Co atoms starting from a bulk CFS lattice (Al has been omitted in our calculations for simplicity due to the similar magnetic moment of pure CFAS and CFS). In the second configuration only one Ge atom is replacing a Co atom, while on the last considered configuration half of the Co sites are occupied by Ge. It can be observed that in the latter case the magnetic moment decreases by 54% compared to the bulk CFAS. It is obvious that calculations presented here are not meant to extensively cover all possible configurations of Ge as a substitutional element in the CFS/CFAS lattice. However this initial set of configurations clearly shows a trend of significant reduction of the magnetic moment per unit cell when Ge is substituting either Co or Fe.

4. Conclusion

We showed that $Co_2FeAl_{0.5}Si_{0.5}$ films deposited at room temperature on Ge(111) substrates have *B2* ordering with magnetic properties strongly dependent on further annealing at a range of temperatures. The decrease of Gilbert damping for the films annealed up to 450 °C indicates improved chemical ordering of $Co_2FeAl_{0.5}Si_{0.5}$. Consequently due to the very similar magnetic moment per unit cell we did not observe any change in saturation magnetisation up to 450 °C. Annealing at higher temperatures drastically changes the magnetic properties of $Co_2FeAl_{0.5}Si_{0.5}$. The saturation magnetisation of the films decreases by nearly 40%, while the coercivity increases almost five-fold when annealed at 525 °C. Equally the ferromagnetic resonance data for films annealed above 450 °C show the presence of magnetically inhomogeneous regions in the annealed films. Atomic resolution imaging and spectroscopy revealed that the changes in magnetic film properties originate from structural changes due to interdiffusion of Ge and $Co_2FeAl_{0.5}Si_{0.5}$, which is directly related to the annealing temperature. First-principles calculations correlate the decrease of the magnetisation with the change of the atomic structure of the CFAS films, mainly *via* substitution of both Fe and Co with Ge. This work clearly shows that forming the desired $L2_1$ phase of CFAS on Ge is hindered by the strong outdiffusion of the Ge into the Heusler film.

Figures:
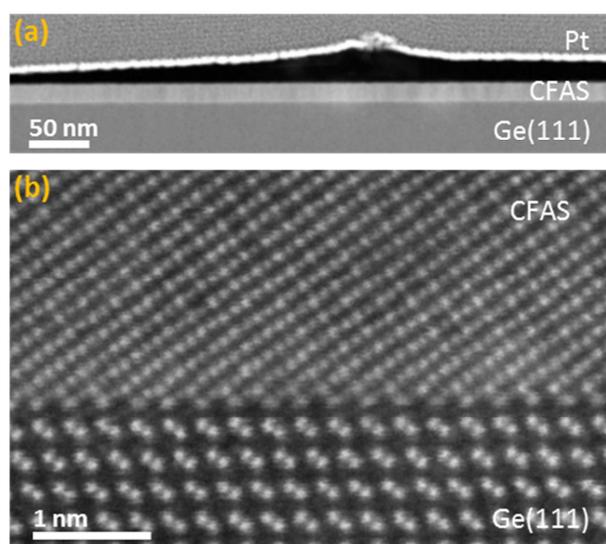
Fig. 1. (a) HAADF STEM image showing that the as-grown film (at RT) is uniform with a thickness of ~18 nm. (b) HAADF STEM image acquired along the $[1\bar{1}0]$ crystallographic direction, showing the abruptness of the CFAS/Ge interface and characteristic of B2 phase.
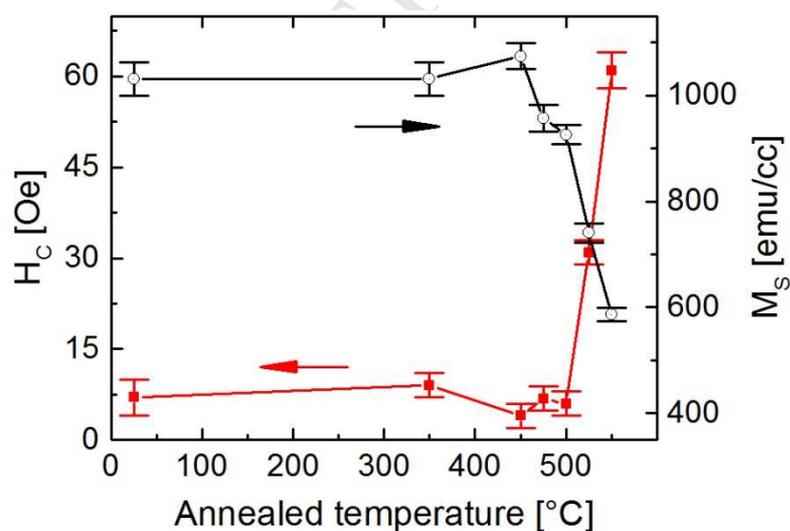
Fig. 2. Saturation magnetization (black hollow circles) and coercivity values (red squares) extracted from hysteresis loops recorded after each annealing condition.
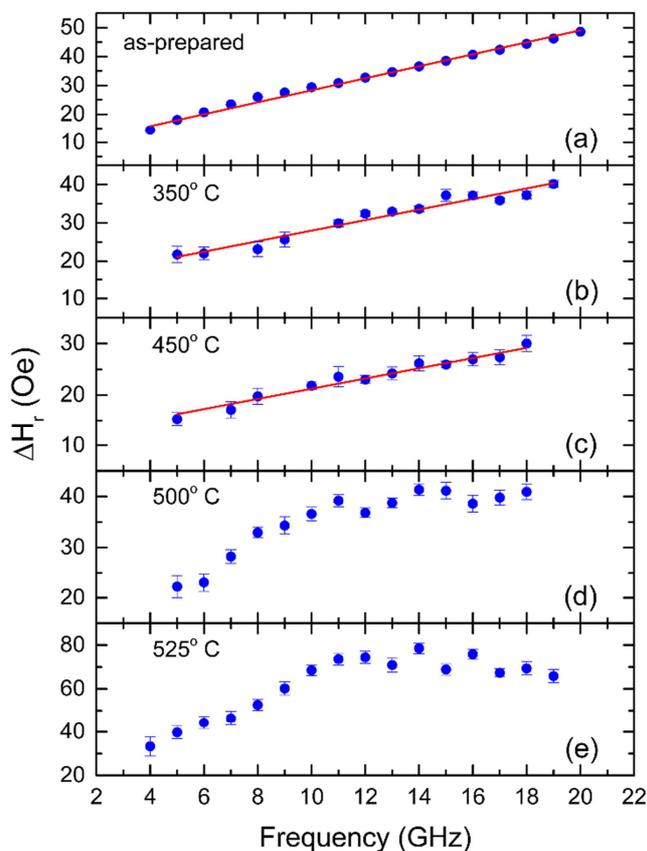
Fig. 3. Resonance field linewidth vs frequency for, (a) as prepared, (b) annealed at 350 °C, (c) at 450 °C, (d) at 500 °C and (e) at 525 °C CFAS/Ge(111).
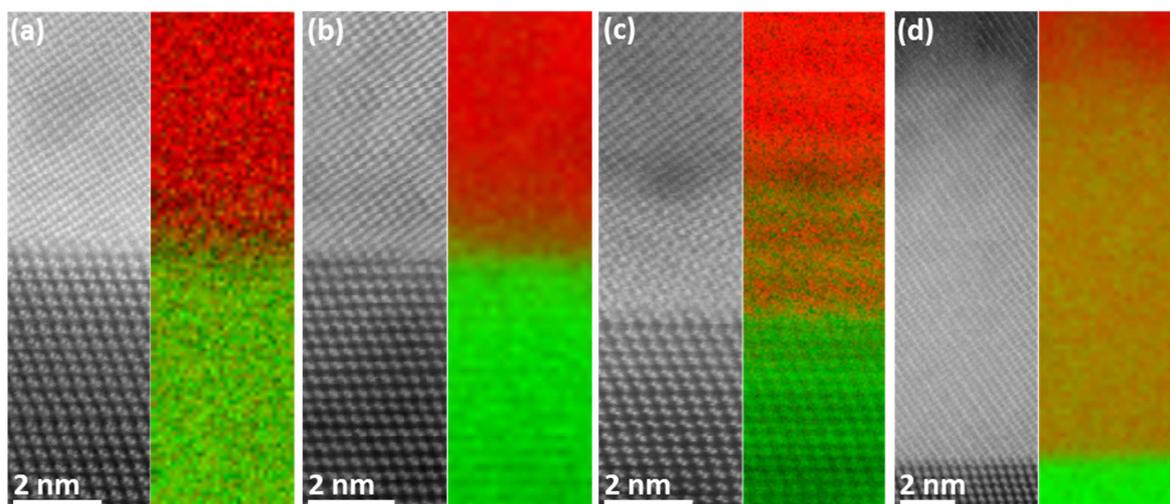
Fig. 4. a) HAADF STEM images paired with corresponding EELS chemical maps across the interface, showing overlaid Co $L_{2,3}$ edge (red) and Ge $L_{2,3}$ edge (green) elemental maps of (a) as-prepared state, after annealing at (b) 350 °C, (c) 500 °C and (d) 550 °C.

n (Ge)	n(Co)	$M\,[\mu_B/\text{unit cell}]$
0	8	24.0
1	7	20.5
2	6	16.9
3	5	15.2
4	4	13.0

Table 1. First-principles calculation results showing the dependence of the magnetic moment *M* as a function of the concentration of Ge substituting Co atoms in CFS. n(Ge) and n(Co) stand for the number of Ge, Fe and Co atoms in a considered configuration. The first row represents bulk CFS where the unit cell has 16 atoms.

References

[1]   S. Bandyopadhyay, M. Cahay, *Introduction to Spintronics*. CRC Press, 2008.

[2]   R. Farshchi, M. Ramsteiner, *J. Appl. Phys.* **113** 19 (2013) 191101, http://dx.doi.org/10.1063/1.4802504

[3]   H. Dery, P. Dalal, L. Cywinski, L. J. Sham, *Nature* **447** 7144 (2007) 573-576, http://dx.doi.org/10.1038/nature05833

[4]   T. Taniyama, E. Wada, M. Itoh, M. Yamaguchi, *NPG Asia Mater.* **3** (2011) 65-73, http://dx.doi.org/10.1038/asiamat.2011.84

[5]   B. Kuerbanjiang, Z. Nedelkoski, D. Kepaptsoglou, A. Ghasemi, S. E. Glover, S. Yamada, T. Saerbeck, Q. M. Ramasse, P. J. Hasnip, T. P. A. Hase, G. R. Bell, K. Hamaya, A. Hirohata, V. K. Lazarov, *Appl. Phys. Lett.* **108** 17 (2016) 172412, http://dx.doi.org/10.1063/1.4948466

[6]   Z. Nedelkoski, B. Kuerbanjiang, S. E. Glover, A. M. Sanchez, D. Kepaptsoglou, A. Ghasemi, C. W. Burrows, S. Yamada, K. Hamaya, Q. M. Ramasse, P. J. Hasnip, T. Hase, G. R. Bell, A. Hirohata, V. K. Lazarov, *Sci. Rep.* **6** (2016) 37282, http://dx.doi.org/10.1038/srep37282

[7]   Z. Nedelkoski, A. M. Sanchez, A. Ghasemi, K. Hamaya, R. F. L. Evans, G. R. Bell, A. Hirohata, V. K. Lazarov, *Appl. Phys. Lett.* **109** 22 (2016) 222405, http://dx.doi.org/10.1063/1.4971281

[8]   Z. Nedelkoski, D. Kepaptsoglou, A. Ghasemi, B. Kuerbanjiang, P. J. Hasnip, S. Yamada, K. Hamaya, Q. M. Ramasse, A. Hirohata, V. K. Lazarov, *J. Phys. Condens. Matter* **28** 39 (2016) 395003, https://doi.org/10.1088/0953-8984/28/39/395003

[9]   I. Žutić, J. Fabian, S. Das Sarma, *Reviews of Modern Physics* **76** 2 (2004) 323-410, https://doi.org/10.1103/RevModPhys.76.323

[10]   M. I. Katsnelson, V. Y. Irkhin, L. Chioncel, A. I. Lichtenstein, R. A. de Groot, *Rev. Mod. Phys.* **80** 2 (2008) 315-378, https://doi.org/10.1103/RevModPhys.80.315

[11]   L. Lari, K. Yoshida, P. L. Galindo, J. Sato, J. Sizeland, D. Gilks, G. M. Uddin, Z. Nedelkoski, P. J. Hasnip, A. Hirohata, M. Oogane, Y. Ando, V. K. Lazarov, *J. Phys. D: Appl. Phys.* **47** 32 (2014) 322003, https://doi.org/10.1088/0022-3727/47/32/322003

[12]   C. Felser, G. H. Fecher, B. Balke, *Angew. Chem. Int. Ed.* **46** 5 (2007) 668-699, http://dx.doi.org/10.1002/anie.200601815

[13]   A. Hirohata, J. Sagar, L. Lari, L. R. Fleet, V. K. Lazarov, (in English), *Appl. Phys. A* **111** 2 (2013) 423-430, http://dx.doi.org/10.1007/s00339-013-7679-2

[14]   N. Tezuka, N. Ikeda, A. Miyazaki, S. Sugimoto, M. Kikuchi, K. Inomata, *Appl. Phys. Lett.* **89** 11 (2006) 112514, http://dx.doi.org/10.1063/1.2354026

[15]   V. K. Lazarov, K. Yoshida, J. Sato, P. J. Hasnip, M. Oogane, A. Hirohata, Y. Ando, *Appl. Phys. Lett.* **98** 24 (2011) 242508, http://dx.doi.org/10.1063/1.3600792

[16]   S. Picozzi, A. Continenza, A. J. Freeman, *Phys. Rev. B* **69** 9 (2004) 094423, https://doi.org/10.1103/PhysRevB.69.094423

[17]   R. Shan, H. Sukegawa, W. H. Wang, M. Kodzuka, T. Furubayashi, T. Ohkubo, S. Mitani, K. Inomata, K. Hono, *Phys. Rev. Lett.* **102** 24 (2009) 246601, https://doi.org/10.1103/PhysRevLett.102.246601

[18]   W. Wang, H. Sukegawa, R. Shan, S. Mitani, K. Inomata, *Appl. Phys. Lett.* **95** 18 (2009) 182502, http://dx.doi.org/10.1063/1.3258069

[19]   N. Tezuka, N. Ikeda, S. Sugimoto, K. Inomata, *Appl. Phys. Lett.* **89** 25 (2006) 252508, http://dx.doi.org/10.1063/1.2420793

[20]   W. Wang, H. Sukegawa, R. Shan, T. Furubayashi, K. Inomata, *Appl. Phys. Lett.* **92** 22 (2008) 221912, http://dx.doi.org/10.1063/1.2940595

[21]   K. Tanikawa, S. Oki, S. Yamada, M. Kawano, M. Miyao, K. Hamaya, *Thin Solid Films* **557** 0 (2014) 390-393, http://dx.doi.org/10.1016/j.tsf.2013.08.128

[22]   S. Yamada, K. Tanikawa, S. Oki, M. Kawano, M. Miyao, K. Hamaya, *Appl. Phys. Lett.* **105** 7 (2014) 071601, http://dx.doi.org/10.1063/1.4893608

[23]   M. Watanabe, E. Okunishi, K. Ishizuka, *Microscopy and Analysis* **23** 7 (2009) 5-7,

[24]   S. J. Clark, M. D. Segall, C. J. Pickard, P. J. Hasnip, M. I. J. Probert, K. Refson, M. C. Payne, *Z. Kristallogr. Cryst. Mater.* **220** (2005) 567-570, https://doi.org/10.1524/zkri.220.5.567.65075

[25]   P. J. Hasnip, J. H. Smith, V. K. Lazarov, *J. Appl. Phys.* **113** 17 (2013) 17B106, http://dx.doi.org/10.1063/1.4801745

[26]   D. E. Parkes, L. R. Shelford, P. Wadley, V. Holý, M. Wang, A. T. Hindmarch, G. van der Laan, R. P. Campion, K. W. Edmonds, S. A. Cavill, A. W. Rushforth, *Sci. Rep.* Article **3** (2013) 2220, http://dx.doi.org/10.1038/srep02220

[27]   M. K. Marcham, L. R. Shelford, S. A. Cavill, P. S. Keatley, W. Yu, P. Shafer, A. Neudert, J. R. Childress, J. A. Katine, E. Arenholz, N. D. Telling, G. van der Laan, R. J. Hicken, *Phys. Rev. B* **87** 18 (2013) 180403, https://doi.org/10.1103/PhysRevB.87.180403

[28]   A. Hrabec, F. J. T. Gonçalves, C. S. Spencer, E. Arenholz, A. T. N'Diaye, R. L. Stamps, C. H. Marrows, *Phys. Rev. B* **93** 1 (2016) 014432, https://doi.org/10.1103/PhysRevB.93.014432

[29]   C. Banerjee, L. M. Loong, S. Srivastava, S. Pal, X. Qiu, H. Yang, A. Barman, *RSC Adv.* **6** 81 (2016) 77811-77817, http://dx.doi.org/10.1039/C6RA05535D

[30]   M. S. Gabor, M. Belmeguenai, T. Petrisor, C. Ulhaq-Bouillet, S. Colis, C. Tiusan, *Phys. Rev. B* **92** 5 (2015) 054433, https://doi.org/10.1103/PhysRevB.92.054433